

Chapter 23

Experimental Study on Seismic Performance of Precast Concrete Shear Wall with Joint Connecting Beam Under Cyclic Loadings

Xilin Lu, Dun Wang and Bin Zhao

23.1 Introduction

Since the advent of the use of precast concrete structural systems, for many decades numerous investigations on the performance and development of novel precast concrete systems have been conducted, such as unbonded post-tensioned precast concrete frame structures (El-Sheikh et al. 1999), unbonded post-tensioned precast concrete walls (Kurama et al. 1999), self-centering precast concrete wall systems with energy dissipators (Restrepo and Rahman 2007) and partially prefabricated laminated composite RC walls (Zhang et al. 2011). Structural connections are a major feature of precast concrete shear walls—distinguished from monolithic shear walls—as they play an important role on the seismic performance and safety of precast concrete shear wall structures, including shear capacity, stiffness and ductility, energy dissipation, and force-transfer (fib Bulletin No. 43 2008). Plenty of studies have been conducted on the performance of precast concrete shear walls with various joint connections (Pekau and Hum 1991; Schultz et al. 1994; Henry et al. 2010). In China, Jiang (Jiang et al. 2011b) first conducted a test on 81 plug-in filled holes for lap-joint steel bar samples, considering factors such as reinforcement bar diameter, concrete strength and anchorage length. These tests were followed by elastic quasi-static tests on a three-story full-scale model using the same connecting method for the steel bars (Jiang et al. 2011b). Qian (Qian et al. 2011) conducted an ex-

X. Lu (✉) · B. Zhao
State Key Laboratory of Disaster Reduction in Civil Engineering, Tongji University,
Shanghai, China
e-mail: lxlst@tongji.edu.cn

B. Zhao
e-mail: binzh@tongji.edu.cn

D. Wang
Research institute of Structural Engineering and Disaster Reduction, Tongji University,
Shanghai, China
e-mail: waltdon77@126.com

perimental study of five wall specimens with an aspect ratio of 2.25, connecting the vertical reinforcement with various splicing techniques such as a single connecting rebar, a mechanic sleeve connection and a sleeve-mortar splicing connection. Ong (Ong et al. 2006) reported the flexural behavior of two precast concrete specimens with one-to-one horizontal loop connections and concluded that an increase in the loop overlapping length, a decrease in the internal diameter, or an overlap spacing of the loop resulted in an increase in the flexural strength of the precast specimen tested. Ma (Ma et al. 2012) conducted an investigation of longitudinal joint details with tight bend diameter U-bars for accelerated bridge construction.

In this paper the concept of a Joint Connecting Beam (JCB) is developed to connect the vertical reinforcement of precast concrete shear walls. The JCB is composed of staggered splicing rectangular steel loops protruding from the wall panel, an assembly of longitudinal steel bars and stirrups, and casted concrete. The influence of the location and height of the JCB on the performance of precast concrete shear walls is studied and comparisons are made with the results of quasi-static tests on monolithic shear walls. The failure mode, the top lateral force-displacement hysteresis curve, lateral strength capacity, deformation, stiffness degradation, reinforcement strains and energy dissipation are presented in detail. The work indicated that the concept and detailing of the JCB are feasible and applicable to precast concrete shear wall structures. Some findings are presented based on the research and suggestions are made for further investigations and engineering applications.

23.2 Experimental Programme

23.2.1 Specimen Design

Seven full-scale wall specimens were designed according to the Chinese code for design of reinforced concrete structures (GB 50010 2010). This included six precast concrete shear walls and a monolithic shear wall. All the wall specimens have the same rectangular section of 1500×200 mm and same concrete strength grade C40. The height of the wall specimens is 2.60 m with a top beam of $400 \times 400 \times 1800$ mm (height and width and thickness) for lateral loading and vertical loading, resulting in an aspect ratio of 2.8 (measured from the bottom of the wall to the centerline of the top beam). The main difference between the precast wall specimens and the monolithic conventional wall is the existence of the joint connecting beam (JCB). The height of the JCB varies with values of 150, 200, 300 mm, chosen to study the effect of the lapped length of steel bars according to the Chinese code (GB 50010 2010). The locations of the JCB are in the middle and at the bottom of the precast wall, with the purpose of checking its role in determining the performance of precast wall. The JCB has the same concrete strength grade C40 of the wall. Detailed information of wall specimens can be found in Table 23.1. All the wall specimens were constructed in a batch at the State Key Laboratory for Disaster Reduction in Civil Engineering of Tongji University. The characteristic values of concrete and steel bars obtained from material property tests are listed in Table 23.2 and 23.3.

Table 23.1 Design parameters of wall specimens

Specimens	Joint connecting beam				Boundary element		Distributed bars	Concrete
	Height (mm)	Location	longitudinal bars	Stirrups	longitudinal bars	Stirrups	Horizontal and vertical	Strength
SW-2	–	–	–	–	6 ϕ 10	ϕ 6@75	ϕ 8@150	C40
PCW-7	150	Bottom	4 ϕ 12	ϕ 6@100	6 ϕ 10	ϕ 6@75	ϕ 8@150	C40
PCW-8	200	Bottom	6 ϕ 10	ϕ 8@100	6 ϕ 10	ϕ 6@75	ϕ 8@150	C40
PCW-9	200	Middle	6 ϕ 10	ϕ 8@100	6 ϕ 10	ϕ 6@75	ϕ 8@150	C40
PCW-10	300	Middle	6 ϕ 10	ϕ 10@100	6 ϕ 10	ϕ 6@75	ϕ 8@150	C40
PCW-11	200	Bottom & Middle	6 ϕ 10	ϕ 8@100	6 ϕ 10	ϕ 6@75	ϕ 8@150	C40
PCW-12	300	Bottom & Middle	6 ϕ 10	ϕ 8@150	6 ϕ 10	ϕ 6@75	ϕ 8@150	C40

Table 23.2 Mean value of concrete properties

Location of Concrete	Cubic Strength	Prism Strength	Modulus of Elasticity (N/mm ²)	Design Strength Grade
	(MPa)	(MPa)		
Precast concrete wall	39.1	26.15	3.33×10^4	C40
Joint connecting beam	38.5	25.81	3.05×10^4	C40

Table 23.3 Mean value of steel bar strength

Diameters	Yielding strength	Ultimate tensile strength	Position of reinforcement	Strength grade
(mm)	(Mpa)	(Mpa)		
6	467.5	607.5	Stirrups A, Ties	HPB300
6	510	620	Stirrups B	HRB400
8	557.5	630	Distributed reinforcement, stirrups B	HRB400
10	552.5	657.5	Reinforcement A and B, stirrups B	HRB400
12	497.5	632.5	Reinforcement B	HRB400

A denotes boundary element; B denotes Joint Connecting Beam (JCB)

23.2.2 Measurement and Test Procedure

Figure 23.1 illustrates the test set-up and the loading history of the wall specimens. A vertical load was first applied to the fixed wall specimens by four hydraulic jacks on top of the loading beam, resulting in an axial force of 1200 kN that was kept constant throughout the entire testing process. A horizontal load was then applied by a Schenck actuator with a 200 mm maximum stroke and 1000 kN capacity, as shown in Fig. 23.1a. A displacement-controlled loading history was exerted on the specimens throughout the entire testing, as shown in Fig. 23.1b. The displacement amplitude of the loading history was applied at 1 mm cycle increments in the elastic range; the yield displacement was determined from the strain of the outermost reinforcement in the boundary element of wall specimen. In the inelastic range displacements were applied at increments equal to the measured yield displacement, with three cycles repeated at each displacement value. The yield displacement for the wall specimens was equal to 8 mm (for PCW-11), 10 and 11 mm (for PCW-12).

Before the start of testing, cracks due to temperature shrinkage during the construction stage along the top interface of the JCB were monitored and marked to distinguish them from cracks due to the damage of specimens during testing. During the entire process of tests, the top displacement, horizontal force, longitudinal and transverse rebar strains, and concrete strains were measured. Displacement of the anchoring beam at the bottom of each wall specimen, which is usually negligible, was also monitored by a displacement transducer, in order to derive the net drift of the wall specimen. In order to monitor the slip displacement between the top interface of the JCB and the precast wall panel above, some additional steel bars with a diameter of 6 mm were installed horizontally in the specimen along the interface of the joint connecting beam and the wall panel above.

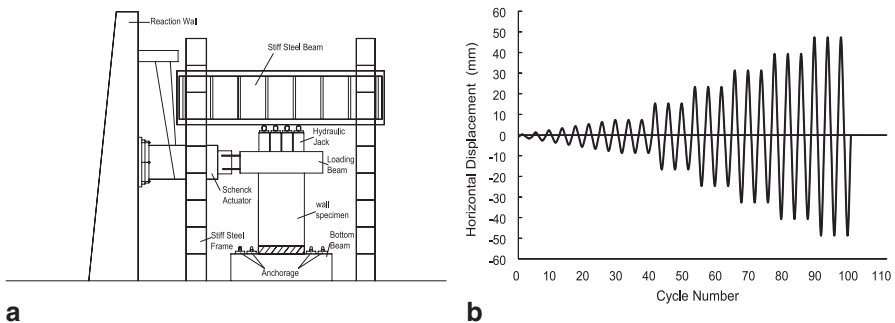


Fig. 23.1 Test set-up and loading history

23.3 Test Results

23.3.1 Overview

The sequence of damage of the wall specimens was observed as follows: at first cracks emerged along the top interface of the JCB and merged with cracks formed during the construction stage, gradually becoming a line. Minor cracks then appeared at the end side and at the bottom of the wall. Vertical cracks occurred at the end and at the middle of the JCB. Meantime, minor slant cracks developed at the corner of the wall and developed upwards. With the increase of lateral displacement, minor spalling of concrete occurred at the top interface of the joint connecting beam, with main diagonal inclined cracks developing both in the pull and push directions. With the increase of vertical cracks and new horizontal cracks in the JCB, concrete at the corner of the wall began to crack severely, resulting in initial spalling of the concrete cover. After reaching the maximum load capacity of the wall specimens, complete spalling of the concrete cover, buckling of the longitudinal rebar and/or fracture of the longitudinal rebars was observed. The test was stopped when the lateral capacity decreased to at least 15% of the maximum load capacity of the wall specimen or when there was a loss of the vertical load bearing capacity. After completion of all tests it was concluded that the failure mode of all wall specimens was a combination of flexure and shear.

Figure 23.2 shows the damage patterns of some typical wall specimens. The drift ratio θ of the wall specimen is defined as the top net displacement divided by the height of the wall specimen. It is observed that when the JCB is located at the bottom of the wall specimen concrete was severely damaged, with complete spalling of the concrete cover of the JCB along a large region (Fig. 23.2a), gap-opening on the top interface of the JCB (Fig. 23.2b and e), minor buckling or no buckling with not fracture of the longitudinal rebar with (Fig. 23.2b and d). When the JCB is located in the middle of the wall specimen, concrete at the bottom damaged severely with spalling of the concrete cover, and buckling and fracture of the longitudinal rebar (Fig. 23.2c), similar to the damage observed for the monolithic wall specimen (Fig. 23.2f).

23.3.2 Hysteresis Behavior and Skeleton Curve

The hysteresis loops of some representative wall specimens are shown in Fig. 23.3. As shown in Fig. 23.3, the characteristics of the hysteresis curves of precast concrete wall specimens are similar to that of the monolithic wall specimen. Initial behavior is practically linear-elastic with few hysteretic cycles developing before appearance of the first cracks. However, with the increase of lateral horizontal displacement after cracks develop, the curve begins to slope down towards the displacement axis, with hysteretic loops of larger area and the pinching effect gradually emerging as

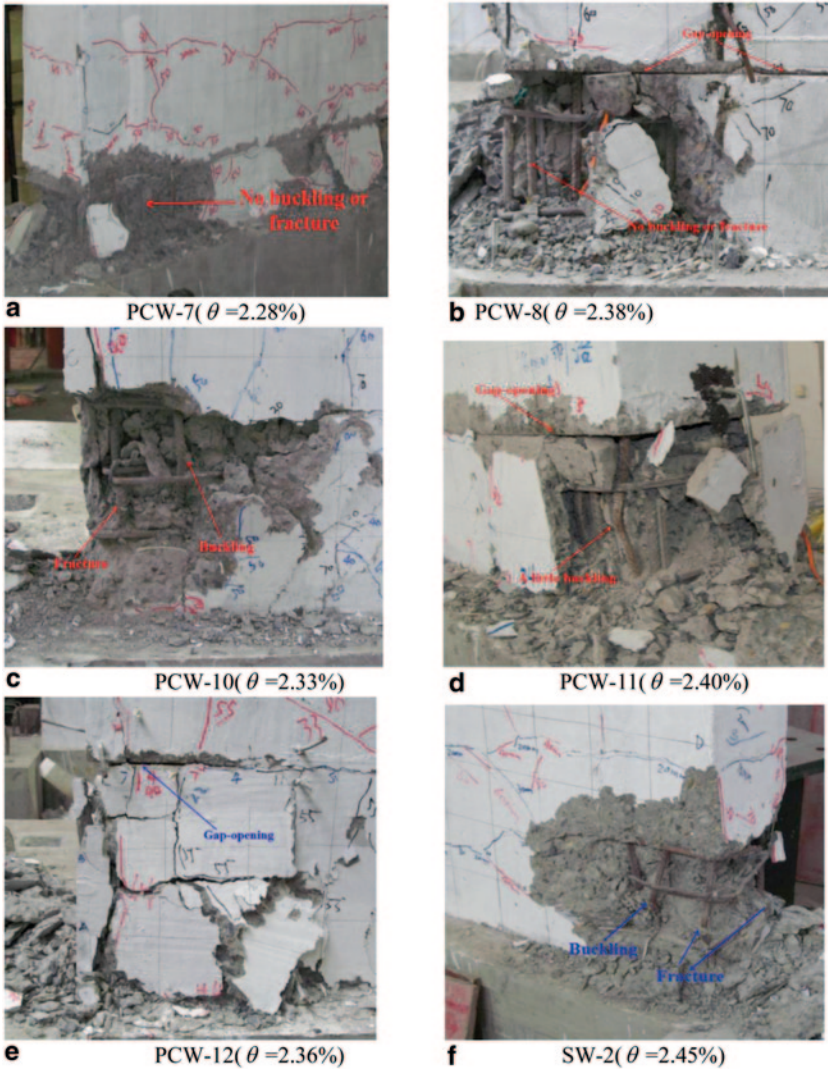


Fig. 23.2 Damage conditions of wall specimens

diagonal cracking develops. The lateral load capacity of wall specimen decreases after reaching the maximum load capacity. The test was stopped due to the loss of vertical load carrying capacity, also demonstrated by the skeleton curves.

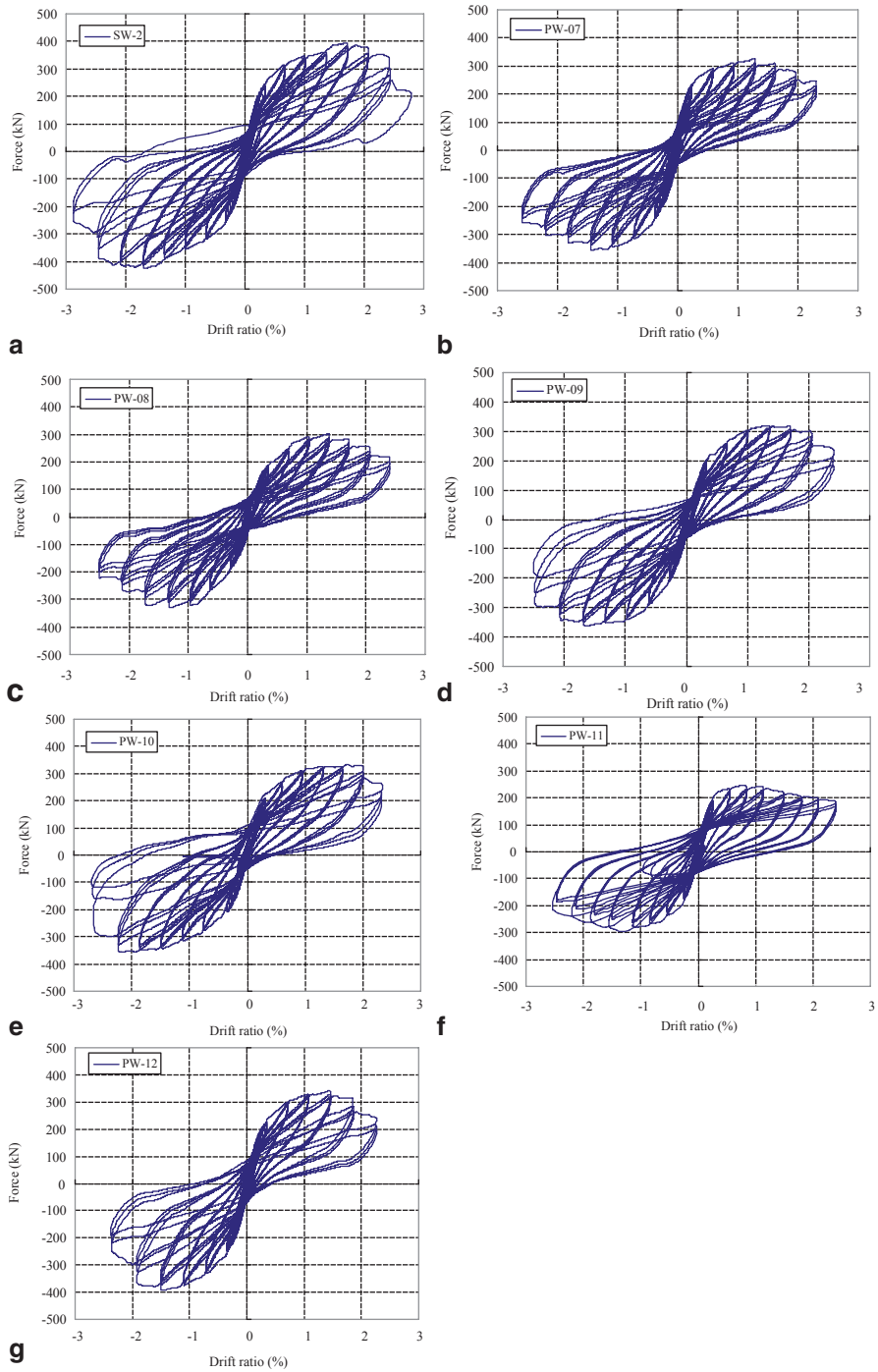


Fig. 23.3 Hysteresis loops of wall specimens

23.3.3 Lateral Strength

Table 23.4 presents the lateral forces of wall specimens in the directions of pull and push at different states, such as cracking, yielding and maximum load capacity. The skeleton curves of the wall specimens are illustrated in Fig. 23.4 and 23.5 and show the ratio of maximum lateral shear strength of precast wall specimens to that of the monolithic wall SW-2. As can be seen from Fig. 23.4 and 23.5, the lateral strength of the precast concrete shear wall with JCB is lower than the lateral strength of the monolithic shear wall, but not lower than 80% (except for PCW-8 and PCW-11). Moreover, with the increase of the height of the JCB when located at the middle of the wall specimens, the lateral strength rises up, with the exception of the case when the JCB is located at the bottom (especially for specimens PCW-8). Further studies are needed on determining how the location of the JCB affects the lateral strength of the shear wall. With smaller heights of the JCB at the bottom of the wall, the precast concrete wall showed the lowest load capacity, such as in specimens PCW-11. This lower capacity of the PCW-11 specimen is attributed to the fact that the PCW-11 specimen was tested for the first time, and to double casting of the JCB. Another reason is a different loading history, with cycles of 8 mm increments applied in the inelastic range.

Table 23.4 Lateral force of wall specimens at various states

Specimens	F_{cr}/kN			F_y/kN			F_{max}/kN		
	Push	Pull	Average	Push	Pull	Average	Push	Pull	Average
SW-2	135.8	144.8	140.3	283.4	297.8	290.6	394.4	426.1	410.25
PCW-7	99	108.1	103.55	237.07	266.27	251.67	325.7	357.7	341.7
PCW-8	89.63	85.47	87.55	222.37	246.2	234.29	301.74	330.21	315.98
PCW-9	84.6	89.2	86.9	232.94	267.5	250.22	319.7	362.4	341.05
PCW-10	87.63	96.48	92.06	241.77	252.88	247.33	333.67	355.9	344.79
PCW-11	131.1	203.9	167.5	188.87	211.07	199.97	245.6	295.6	270.6
PCW-12	97.02	93.48	95.25	246.27	280.69	263.48	391.68	340.59	366.14

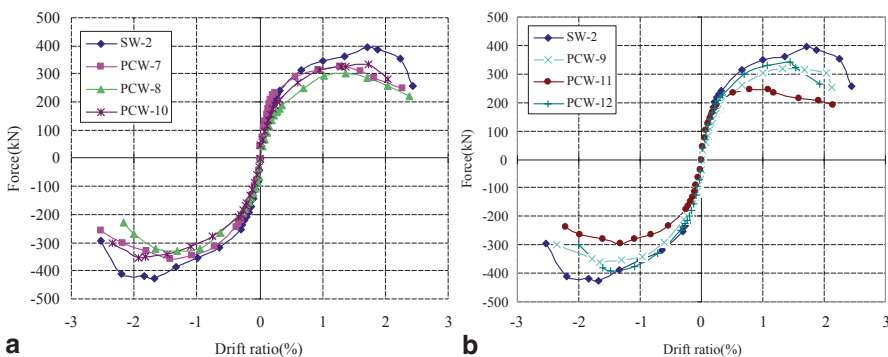


Fig. 23.4 Skeleton curves of wall specimens

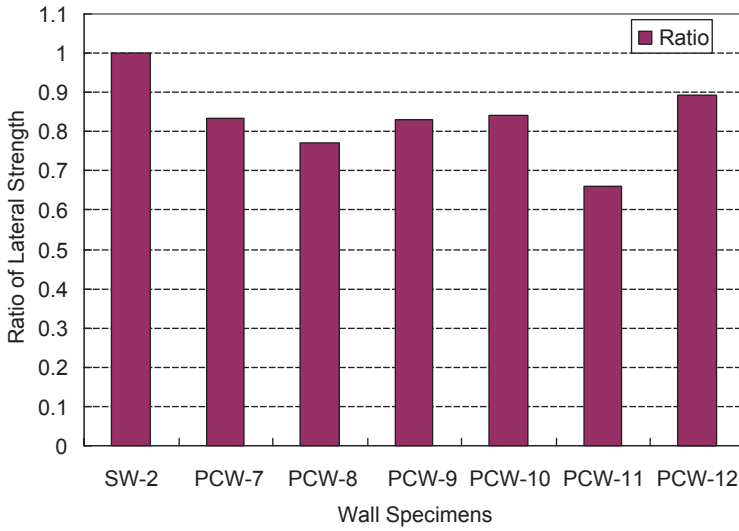


Fig. 23.5 Ratio of lateral strength of wall specimens

23.3.4 Ductility Evaluation

Ductility characterizes the capacity of a structure or member to deform without significant degradation of its loading capacity, and is generally defined by the so-called displacement ductility coefficient μ_{Δ} :

$$\mu_{\Delta} = \Delta_u / \Delta_y \quad (23.1)$$

where Δ_u and Δ_y are the ultimate and yield deformations. As mentioned by many researchers (Chen et al. 2009), different definitions may result in a remarkable difference in the displacement ductility coefficient. In this paper, the yield displacement during the test used for the loading history was determined by the first yield strain of the outermost longitudinal reinforcement in the boundary element of the wall specimen. The yield displacement for calculating the displacement ductility coefficient was determined by a combination of the Park-method (Park 1989) and the method of equivalent energy of ASTM ES2126-02a (ASTM 2003). It was found that there are some differences in the yielding displacement calculated according to these formulas, yet not listed here. That the displacement ductility coefficient μ_{Δ} was computed following the expression:

$$\mu_{\Delta} = \frac{|\Delta_u| + |-\Delta_u|}{|\Delta_y| + |-\Delta_y|} \quad (23.2)$$

Table 23.5 Deformation of wall specimens at various states and ductility

Specimens	Δ_{cr}/mm			Δ_y/mm			Δ_u/mm			Ductility	
	Push	Pull	Average	Push	Pull	Average	Push	Pull	Average	μ_Δ	$\xi(\Delta_u)$
SW-2	3.5	2.8	3.15	14.49	15.21	14.85	63.97	65.53	64.75	4.36	0.808
PCW-7	1.9	2.2	2.05	7.11	13.45	10.28	53.96	60.49	57.23	5.57	0.824
PCW-8	3.53	0.89	2.21	15.31	15.08	15.2	57.32	54.15	55.74	3.68	0.826
PCW-9	1.3	3.2	2.25	14.15	14.37	14.26	58.5	62.63	60.57	4.25	0.855
PCW-10	2.19	2.51	2.35	13.07	16.74	14.91	59.94	65.27	61.11	4.1	0.815
PCW-11	2.2	2.3	2.25	6.82	11.82	9.32	50.01	58.77	54.39	5.83	0.899
PCW-12	2.02	2.13	2.08	12.43	13.63	13.03	49.1	51.17	50.14	3.85	0.882

Considering the complexity and different definitions of the yield displacement, a new index of the ductility factor is adopted in this paper to evaluate the ductility characteristics of wall specimens. The relative strain energy $\xi(\Delta_u)$ is defined as follows (fib Bulletin 2008):

$$\xi(\Delta_u) = W_{\text{int}}(\Delta_u) / (F_{\text{max}} \Delta_u) \quad (23.3)$$

where $W_{\text{int}}(\Delta_u)$ is the area defined by the load-displacement relationship of the wall specimen at ultimate displacement and F_{max} is the maximum load capacity of the wall specimen. Values of the ductility factor for different indices are listed in Table 23.5, showing that the ductility of precast wall specimens is slightly superior to that of a monolithic wall specimen.

23.3.5 Strain Distribution of Reinforcements

The strain distribution of reinforcement in the boundary element, 20 mm above the bottom cross section of the wall specimen is shown in Fig. 23.6 for the 2 mm, 10 mm (8 mm for PCW-11, 11 mm for PCW-12) and 30 mm (24 mm for PCW-11, 33 mm for PCW-12) loading in the pull direction, which corresponds approximately to the cracking stage, the yield stage and occurrence of the main diagonal cracks, respectively. It is noted that the plane-section assumption holds for all the wall specimens before the yielding stage, thereafter, for the wall specimens with the JCB at the bottom, the plane-section assumption is no longer maintained when compared with the other wall specimens. Moreover, none of the walls (regardless of the location and height of the JCB and for the monolithic wall specimens SW-2) conform

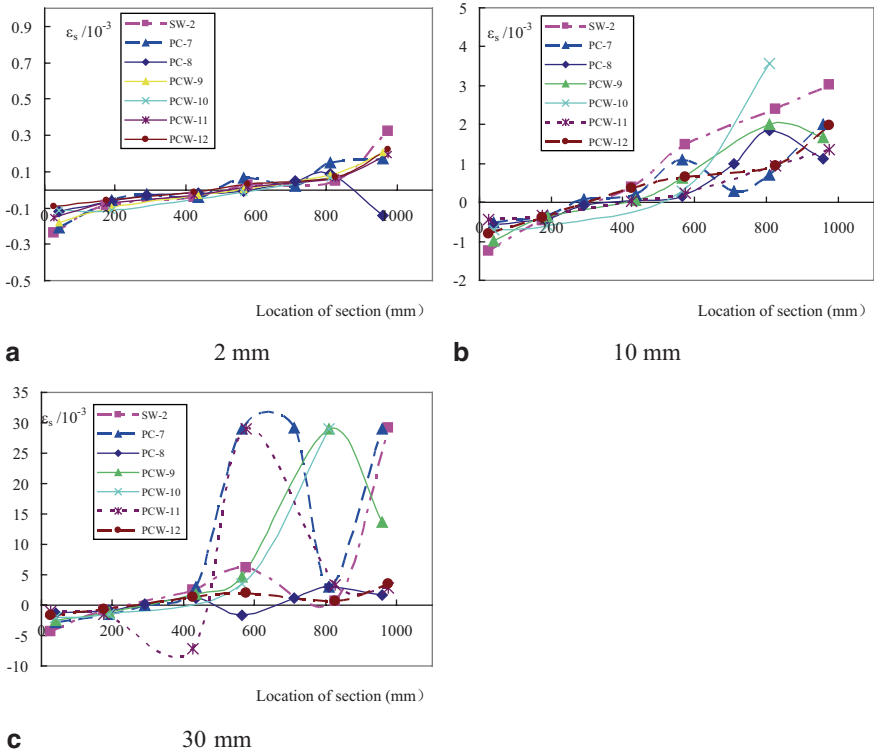


Fig. 23.6 Strain reinforcement distribution of boundary elements at different loading states

with the plane-section assumption at sustained levels of loading after yielding and formation of the main diagonal cracks.

23.3.6 Energy Dissipation

The energy dissipation of the wall specimens with the increase of lateral displacement is calculated by calculating the area under the force-displacement curves as shown in Fig. 23.7. The curves show that prior to yield (i.e. 10 mm), a very small amount of energy is dissipated. After that, a larger amount of energy is dissipated as displacements increase (except for PCW-12). When the JCB is located at the bottom, precast wall specimens dissipate less energy than a monolithic shear wall. When the JCB is located in the middle of the wall, the energy dissipation of wall all specimens is nearly the same. The height of the JCB seems not to have a primary influence on the energy dissipation of wall specimens.

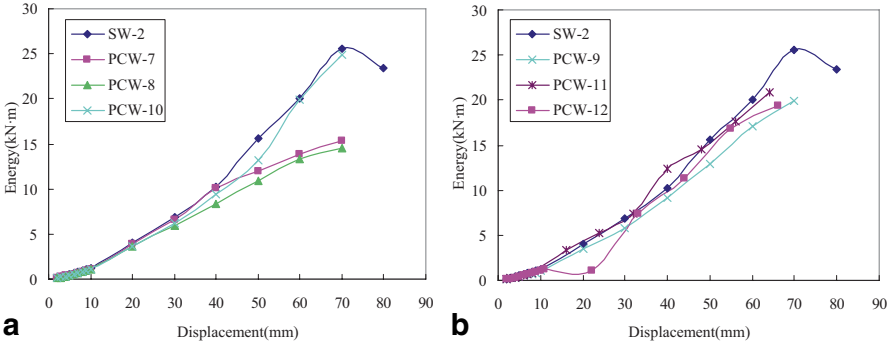


Fig. 23.7 Energy dissipation of all the wall specimens

23.3.7 Stiffness Degradation

Stiffness K_i is defined as the secant stiffness of a wall specimen at the maximum displacement of each cycle under cyclic lateral displacement(JGJ101-96 1996); the calculation formula is as follows:

$$K_i = \frac{|F_i| + |-F_i|}{|\Delta_i| + |-\Delta_i|} \tag{23.4}$$

where F_i is the maximum force during the i th cycle, and Δ_i is the horizontal displacement corresponding to the maximum force. The positive and negative signs represent the direction of pull and push, respectively. It is clearly demonstrated from Fig. 23.8 that stiffness degradation of all wall specimens is nearly the same, especially in the inelastic stage, with a few differences in the elastic stage, regardless of the location and the height of the JCB.

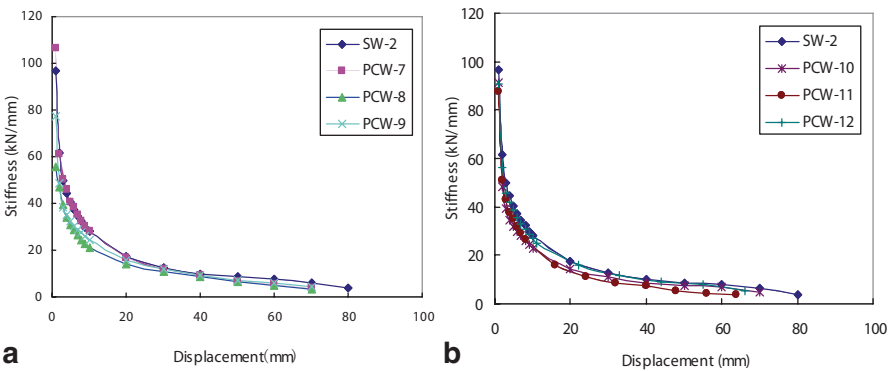


Fig. 23.8 Stiffness degradation of wall specimens

23.4 Conclusions

In this paper, six precast concrete shear wall members with a Joint Connecting Beam (JCB) were designed according to the current seismic Chinese design code. Cyclic tests were conducted at the State Key Laboratory of Disaster Reduction in Civil Engineering, Tongji University. The following conclusions are drawn after comparative analysis of the test results:

- The failure mode of the precast wall with the JCB specimen is similar to that of a monolithic wall specimen, which includes flexural-shear failure with crushing of concrete at the bottom, tensile yield or buckling, and in some cases fracture of vertical reinforcement in the boundary elements, all these observed when the JCB is located in the middle of the wall specimen.
- The lateral load capacity of precast wall specimens with the JCB is lower than that of a monolithic shear wall, not exceeding 20%, except for the PCW-11 specimen. The height and location of the JCB have an important role in the strength of the specimen, the bigger the height of the JCB, the higher the strength of the wall specimen. For JCBs located at the bottom of the wall adverse conditions are found, especially for smaller heights due to the existence of a plastic hinge region. By using higher strength concrete and steel fiber concrete, this situation may be improved. The deformation of precast walls with JCB is slightly smaller and occurs earlier than for the monolithic case; however, the ductility of precast walls with JCB is superior to that of a monolithic wall, as confirmed by the index of relative strain energy. The higher the height of the JCB, the lower the ductility found in the precast walls. Energy dissipation and stiffness degradation of precast walls with JCB are similar to those of monolithic wall specimens, regardless of the location of JCBs.
- The concept of the joint connecting beam is feasible and effective. It can effectively transfer stresses in the reinforcement of the wall above and below the JCB. However, further studies are needed such as the use of high quality JCBs to improve the performance of precast concrete walls, so as to promote the application of precast concrete walls with joint connecting beams.

Acknowledgments The financial supports from the Key Technology R&D Program for the 12th 5-year Plan of China under Grants No. 211BAJ09B01-03 are gratefully acknowledged.

References

- ASTM (2003) Standard test method for cyclic (Reversed) load test for shear resistance of walls for buildings, ES 2126-02a
- Chen LZ, Lu XL, Jiang HJ, Zheng JB (2009) Experimental investigation of damage behavior of RC frame members including non-seismically designed columns. *Earthq Eng Eng Vib* 8(2):301-311

- El-Sheikh M, Sause R, Pessiki S, Lu L-W (1999) Seismic behavior and design of unbonded post-tensioned precast concrete frames. *PCI J* 44(3):54–71
- Fédération internationale du béton, Fédération internationale du béton (2008) Task Group 6.2, Structural Connections for Precast Concrete Buildings. *fib Bulletin No. 43.*, the International Federation for Structural Concrete (*fib*), 2008
- GB 50010 (2010) The code for design of concrete structures of China
- Henry R, Aaleti S, Sritharan S, Ingham J (2010) Concept and finite-element modeling of new steel shear connectors for self-centering wall systems. *J Eng Mech* 136(2):220–229
- Jiang HB, Chen ZX, Zhang JQ et al (2011a) Quasi-static test of precast reinforced concrete shear wall structure. *J Build Struct* 32(6):34–40 (in Chinese)
- Jiang HB, Zhang HS, Liu WQ et al (2011b) Experimental study on plug-in filling hole for steel bar anchorage of the PC structure. *J Harbin Inst Technol* 43(4):28–36 (in Chinese)
- JGJ101-96 (1996) Specification of test methods for earthquake resistant building of China
- Kurama Y, Sause R, Pessiki S, Lu LW (1999) Lateral load behavior and seismic design of unbonded post-tensioned precast concrete walls. *ACI Struct J* 96(4):622–633
- Ma ZGJ, Cao Q, Chapman CE, Burdette EG, French CEW (2012) Longitudinal joint details with tight bend diameter U-bars. *ACI Struct J* 109(6):815–824
- Ong KCG, Hao JB, Paramasivam P (2006) Flexural Behavior of precast joints with horizontal loop connections. *ACI Struct J* 103(5):664–671
- Park R (1989) Evaluation of ductility of structures and structural assemblages from laboratory testing. *Bull New Zealand Natl Soc Earthq Eng* 22(3):155–166
- Pekau OA, Hum D (1991). Seismic response of friction jointed precast panel shear walls. *PCI J*, 36(2):56–71
- Qian JR, Yang XK, Qin H (2011) Tests on seismic behavior of pre-cast shear walls with various methods of vertical reinforcement splicing. *J Build Struct* 32(6):51–59 (in Chinese)
- Restrepo J, Rahman A (2007) Seismic performance of self-centering structural walls incorporating energy dissipators. *J Struct Eng* 133(11):1560–1570
- Schultz AZ, Mafana RA, Tadros MK (1994) Experimental study of joint connections in precast concrete walls. Fifth U.S. National Conference on Earthquake Engineering, Vol II, 1994
- Zhang HM, Lu X L, Duan YF (2011) Experimental study and numerical simulation of partially prefabricated laminated composite RC walls. *Adv Struct Eng* 14(5):967–979